



## ENGINEERING SCIENCES

# Specific surface area of polydispersions as a function of size distribution sharpness

PAULO FILIPE T. LOPES, JOSÉ AURÉLIO M. DA LUZ & FELIPE O. MILHOMEM

**Abstract:** Knowledge of particulate system properties is very important in various industrial instances and the possibility of fast predicting the behavior of such systems is an important control tool. The specific surface area of simulated particulate systems was studied as a function of the sharpness parameter of the size distribution of the Gates–Gaudin–Schumann, Gaudin–Meloy and Rosin–Rammler equations. The results showed good statistical adherence, especially the Rosin–Rammler equation, in situations where it is the best descriptor of particle size distribution.

**Key words:** particle size distribution, sharpness index, statistical distribution, surface area.

## INTRODUCTION

Specific surface area of granular media (bulk material in general) plays a relevant role in various instances of engineering, such as reactors with solid/liquid, liquid/gas, or solid/gas systems. However, this parameter is generally difficult to quantify, especially when speed in its determination is required (as in the case of its use as input in algorithms for dynamic online process control). Instrumental techniques, such as  $N_2$  adsorption (in accordance with the BET isotherm), liquid porosimetry, or X-ray tomography, are usually costly, time-consuming and sometimes unfeasible in the environment of a production process. Therefore, indirect and quick techniques for determining the specific surface area become very attractive. The development of a tool for inference of this parameter, based on the particle size distribution of the particulate medium, was the motivation for the present work.

Particle size distribution of granular media can commonly be described appropriately by

equations, with behavior similar to a lognormal particle size distribution (Gaussian curve for argument logarithm) (Allen 1981, Bender 2000). Generally, however, other statistical distributions are used, either for greater statistical adherence or for more convenient algebraic manipulation simplicity (since distributions derived from the Gaussian distribution are not Riemann integrable).

Statistical distributions currently used in the analysis of particulate systems (in various instances such as minerometallic, chemical, ceramic, food and other processes) are, for example, Gates–Gaudin–Schumann (GGs), Gaudin–Meloy (GM) and Rosin–Rammler (RR). They are given by equations 1, 2 and 3 of Table I.

In addition to the knowledge on its own of the particle size characteristics and its influence on size-dependent operations, the data obtained from such features can be used in other instances, such as relating the friction angle to the bulk material's size distribution. (Edil et al. 2007), predicting soil water retention (Mohammadi & Meskini-Vishkaee 2012, Nasta et

**Table I. Usual distributions for characterization of polydisperse systems (real argument  $x$  is particle size).**

Tag	Accumulated passing ( $Y(x)$ )	Parameters	Eq.
GGS	$Y(x) = \left(\frac{x}{x_{max}}\right)^n$	$n$ – distribution exponent; $x_{max}$ – top size.	(1)
GM	$Y(x) = 1 - \left(1 - \frac{x}{x_{max}}\right)^n$	$n$ – distribution exponent; $x_{max}$ – top size.	(2)
RR	$Y(x) = 1 - \exp\left[\ln\left(\frac{1}{2}\right) \times \left(\frac{x}{x_{50}}\right)^n\right]$	$n$ – sharpness (uniformity coefficient); $x_{50}$ – median diameter.	(3)

al. 2009), determining porosity (Ouchlyama & Tanaka 1986, Valadares & Da Luz 2004) and bed permeability (Liu et al. 2019), as well as predicting particle breakage during comminution (Epstein 1948, King 2001) – just to quote a few cases.

Another interesting example is the interrelationship between specific surface of aggregates and their degree of packing, with impact on concrete properties such as mortar workability and strength of cured concrete (Hunger & Brouwers 2009). The specific surface area computed from the measured particle size distributions and its corresponding value estimated by Blaine permeabilimetry has revealed a constant ratio and could be used to predict the quality of the concrete. Ultimately, the specific surface area and particle shape affect the flowability and water requirement of Portland cement mortar. Working on this line, Ghasemi et al. (2018) calculated the specific area of granular systems as a function of particle size curves and particle morphometric modeling (assuming polyhedral particle shapes).

In the present study, the equations in Table I were used to simulate particle size distributions of hypothetical particulate

systems by varying the sharpness parameter ( $n$ ) and correspondingly calculating the resulting volumetric specific surface area ( $s_v$ ). Thus, it was possible to generate a cloud of ordered  $n$  versus  $s_v$  pairs, of sufficient magnitude to allow the mathematical prediction of volumetric specific surface area of particulate systems only on the basis of statistical parameters of their distributions descriptors, as discussed below.

### MODELING THE PROBLEM

The specific volumetric surface area of a particle is the ratio between its area and its volume. For spherical particles the solution is trivial. In the case of morphologically irregular particles, one can consider the equivalence of the particle to a sphere of the same dimensions (in terms of diameter, projection area, volume, etc.), by adopting appropriate morphometric coefficients (for sphere:  $k_s = k_v = 1$ ). The specific volume surface area  $s_v$  of an irregular particle (from a size class  $i$ ) is then equal to:

$$s_v = \frac{\text{particle surface area}}{\text{particle volume}} = \frac{A}{V} = \frac{\alpha_s \times x_i^2}{\alpha_v \times x_i^3} = \frac{k_s \times \pi \times x_i^2}{k_v \times \frac{\pi}{6} \times x_i^3} = \frac{k_s \times 6}{k_v \times x_i} \quad (4)$$

This demonstrates the dependence of volumetric surface area on particle size ( $x$ ), tending to very low values for very large particles and infinite value for very tiny particles.

It is convenient to mention morphometric coefficients often vary with the particle size class. A classic compilation by Orr Jr. & DallaValle (1959) can be cited to illustrate this phenomenon, shown in Table II and Figure 1, where the values of morphometric coefficients of quartz sand and crushed quartz are compared. Quartz particles (mineral free of cleavage planes) subjected to natural transport and physical weathering processes tend to decrease their sphericity with increasing size. On the other hand, artificially comminuted particles increase their irregularities with increasing degree of comminution (smaller particles tend to be more irregular).

The masses of particles retained in each size class,  $i$  (where  $x_i > x_{i+1}$ ), can be calculated from the frequency ( $f_i$ ), whereas the approximate number of particles ( $N_i$ ) is obtained by dividing the retained volume in each class by the volume of the average particle of this class. Thus, it results:

$$f_i = Y(x_i) - Y(x_{i+1}) = \frac{m_i}{m_t} \therefore m_i = m_t \times f_i \quad (5)$$

$$N_i = \frac{\frac{m_i}{\rho}}{k_v \times \frac{\pi}{6} \times x_i^3} \quad (6)$$

$$N_i = \frac{6}{k_v \times \pi} \times \frac{m_i}{\rho \times x_i^3} = \frac{6}{k_v \times \pi} \times \frac{m_i \times f_i}{\rho \times x_i^3} \therefore N_i = \frac{6}{k_v \times \pi} \times \frac{V_i \times f_i}{x_i^3} \quad (7)$$

Taking into account the amount of particles of each class ( $N_i$ ), the expression for calculating the specific volumetric surface area becomes:

$$s_v = \frac{\sum k_s \times \pi \times x_i^2 \times N_i}{\sum \frac{k_v \times \pi}{6} \times x_i^3 \times N_i} \quad (8)$$

**Table II. Surface and volume shape coefficient for some particulate materials (modified data from Orr Jr. and DallaValle's).**

Granular system	$x_{50}$ [m]	Shape coefficient	Primary data source (apud Orr Jr. & DallaValle, 1959)
White sand	$2.90 \times 10^{-3}$	$k_s = 0.668$	DallaValle (1938)
White sand	$8.00 \times 10^{-4}$	$k_s = 0.859$	DallaValle (1938)
White sand	$4.00 \times 10^{-4}$	$k_s = 0.828$	DallaValle (1938)
Filter sand	$6.00 \times 10^{-4}$	$k_s = 0.859$	DallaValle (1938)
Filter sand	$5.00 \times 10^{-4}$	$k_s = 0.923$	DallaValle (1938)
Crushed quartz	$8.30 \times 10^{-3}$	$k_s = 0.796$	Martin (1927-8)
Crushed quartz	$4.90 \times 10^{-3}$	$k_s = 0.796$	Martin (1927-8)
Crushed quartz	$1.10 \times 10^{-3}$	$k_s = 0.700$	Martin (1927-8)
Crushed quartz	$3.00 \times 10^{-4}$	$k_s = 0.668$	Martin (1927-8)
Crushed quartz	$2.20 \times 10^{-3}$	$k_v = 0.535$	Martin (1927-8)
Crushed quartz	$1.90 \times 10^{-3}$	$k_v = 0.325$	Goldman & DallaValle (1939)
Crushed quartz	$8.90 \times 10^{-4}$	$k_v = 0.286$	Goldman & DallaValle (1939)
Crushed quartz	$4.90 \times 10^{-4}$	$k_v = 0.516$	Martin (1927-8)
Crushed quartz	-	$k_v = 0.267$	Hatch & Choate (1929)
Calcite	-	$k_v = 0.258$	Hatch & Choate (1929)
Hornblende	$5.00 \times 10^{-5}$	$k_v = 0.038$	Goldman & DallaValle (1939)
Dolomite	$4.00 \times 10^{-5}$	$k_v = 0.363$	Goldman & DallaValle (1939)
Feldspar	$4.00 \times 10^{-5}$	$k_v = 0.497$	Goldman & DallaValle (1939)

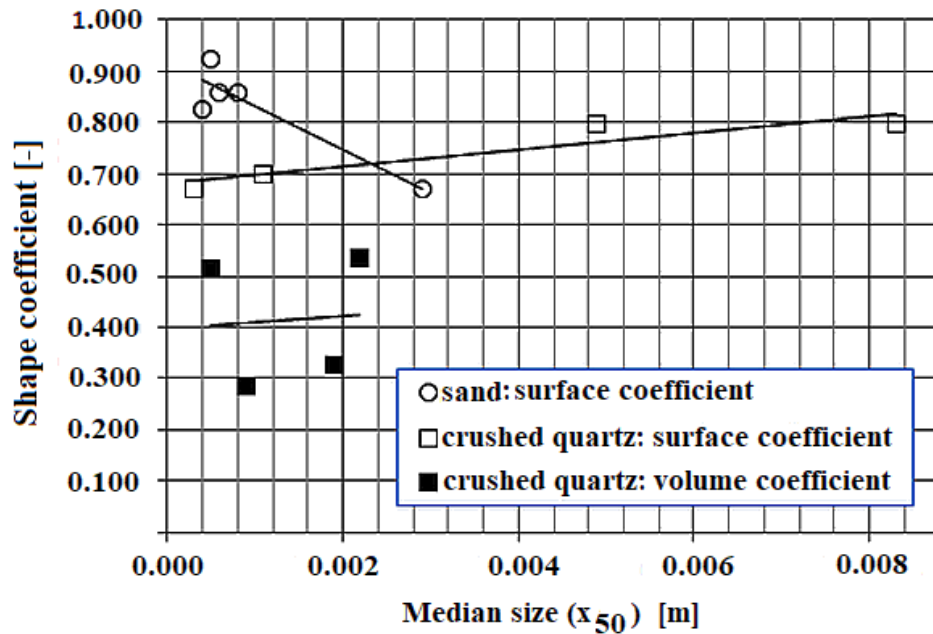


**Figure 1.** Variation of shape coefficients as a function of particle size and provenance (data from Table II).

Substituting equation (10) into (4) finally results:

$$s_v = 6 \times \sum_{i=1}^m \frac{k_s \times f_i}{k_v \times x_i} = s_m \times \rho \tag{9}$$

In the previous equation  $s_m$  is the specific mass surface area (expressed in  $m^2/kg$ ) and  $r$  is the particle’s density (expressed in  $kg/m^3$ ). The simulations were performed based on the above, adopting spherical particles ( $k_s = k_v = 1$ ), and generating a size distribution with relative size ranging from 0 to 1 (with increments of 0.0025).

The mass cumulative pass-through proportion ( $Y(x)$ ) was simulated for distributions described by GGS, GM and RR equations. The exponent values of the distributions were in the range:  $0.001 \leq n \leq 100$ . Although such extreme limits are not usual in industrial reality, they were taken into account for a broader range of results. Based on cumulative mass function, the retained fraction in each size class was determined and, accordingly, the specific surface area of each fraction was calculated. The specific

surface areas for the simulated distributions were obtained from the sum corresponding to all granulometric classes.

Once in possession of the specific surface area values for the tested values of  $n$ , the regression between sharpness parameter and volumetric surface area was performed, thus making it possible to obtain a general equation to predict the surface area based on  $n$ .

## RESULTS

Figure 2 illustrates the surface area curves versus the exponent of the distribution. Similar behavior of Gates–Gaudin–Schumann and Rosin–Rammler distributions was observed: small initial values, for small values of  $n$ , which increase until they decrease again, when the exponent is greater than 1, decreasing asymptotically. In contrast, for Gaudin–Meloy distribution a gradual increase in surface area is observed as the exponent increases, tending to asymptotic saturation.

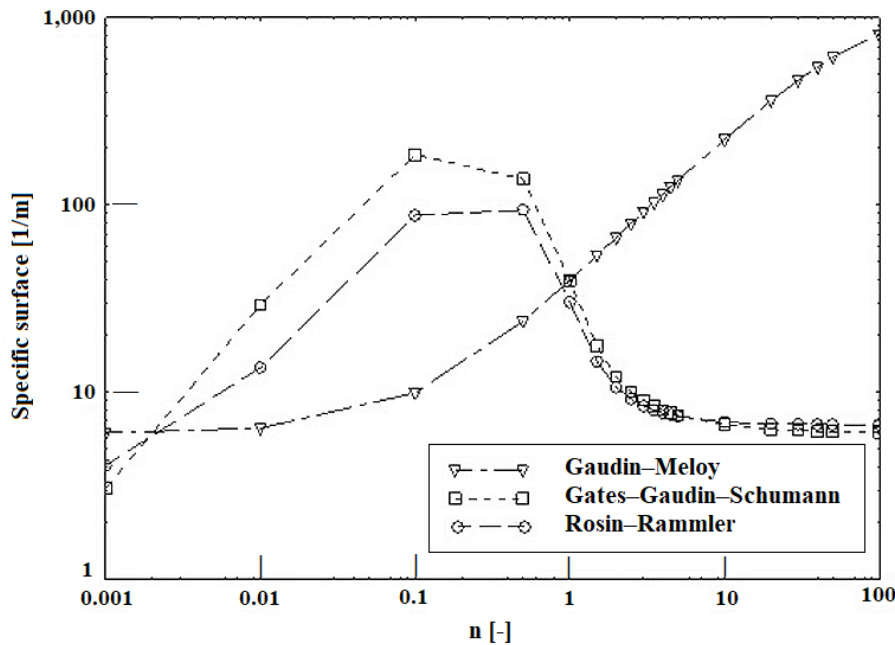


**Figure 2.** Specific volumetric surface area of spheroidal systems as a function of exponent *n*.

A regression analysis was performed from the simulated values, using nonlinear regression with *Easyplot* software. Table III systematizes the predicted equations of the specific surface area of polydisperse spheroidal particulate systems as a function of the distribution exponent. Using literature results (da Luz 2005), one can immediately calculate the surface area of the granular system which is well described by the modified logistic equation (de Lynch-Rao’s equation), shown below (Eq. 13).

$$Y = \frac{e^{\beta \times \left(\frac{x}{x_{50}}\right)} - 1}{e^{\beta \times \left(\frac{x}{x_{50}}\right)} + e^{\beta} - 2} \tag{13}$$

In possession of the parameter  $\beta$ , the sharpness index (*n*) of the “equivalent” Rosin-Rammler equation can be calculated straightforwardly and the value obtained can be applied into equations (12), (12a) and (12b). According da Luz (2005), the relationship between the two sharpness parameters is expressed by:

$$\beta = 34.555 \times e^{\left(\frac{3.9}{n^{0.5984}}\right)} \tag{14}$$

Another aspect to be highlighted is that in Gaudin-Meloy and Gates-Gaudin-Schumann distributions there is a confounding effect between the central tendency parameter and the dispersion parameter, both embedded in the distribution exponent (since the second parameter in the equation refers to the top size). Thus, concomitant change in the distribution median occurs when parameter *n* is modified, logically indicating the exponent cannot be interpreted as an isolated measure of the degree of uniformity of sizes (often referred to as sharpness). In contrast, Rosin-Rammler distribution shows total independence of the two parameters, since they are unambiguously explicit in the equation, which facilitates the analysis of the behavior of particulate systems occurring in industrial practice. By the way, the usual range of sharpness in industry applications is:  $0.5 \leq n \leq 4.0$ .

**Table III. Equations and parameters from nonlinear regression.**

Distribution	Regression equations	Fitting parameters	Equation
GM	$s_v = a \times [1 - \exp(-b \times n^c)]$	$a = 1022.79$ $b = 0.0385428$ $c = 0.808936$ Coefficient of determination: $R^2 = 0.99991$	(10)
GGs	$s_v = \left[ a \times k \times b^a \times n^{\frac{(a-1)}{(n^a + b^a)^2}} \right] + c$	$a = 1.9592$ $b = 0.38077$ $c = 6.4148$ $k = 144.129$ Coefficient of determination: $R^2 = 0.99905$	(11)
RR	$s_v = a(n) \times d_{50}^{-b(n)}$ (12)	$a(n) = \frac{290.0568 \times n^{1.65813}}{(n^{1.65813} + 0.20708^{1.65813})} + 6$ Coefficient of determination: $R^2 = 0.99910$	(12a)
		$b(n) = 1 - \exp\left(-\left(\frac{n}{0.67235}\right)^{1.46902}\right)$ Coefficient of determination: $R^2 = 0.99970$	(12b)

## CONCLUSIONS

The equations obtained here for the prediction of the specific surface area of particulate systems accurately described by the Rosin–Rammler, Gates–Gaudin–Schumann and Gaudin–Meloy statistical distributions (and, furthermore, by modified logistic distribution) allow the rapid implementation of process monitoring and control algorithms, in various instances of engineering, where specific surface area plays a relevant role, such as chemical reactors with solid/liquid, liquid/gas, or solid/gas systems, filtration circuits, solvent extraction processing routes, formulation of Portland cement mortars, adsorption processes, and fines agglomeration operations, just to name a few.

## Acknowledgments

The authors are grateful to the Conselho Nacional de Desenvolvimento Científico e Tecnológico (CNPq), Fundação de Amparo à Pesquisa do Estado de

Minas Gerais (FAPEMIG), and the Coordenação de Aperfeiçoamento de Pessoal de Nível Superior (CAPES) for their financial support of this work.

## REFERENCES

- ALLEN T. 1981. Particle Size Measurement, 3<sup>rd</sup> ed., Springer, 678 p.
- BENDER EA. 2000. An Introduction to Mathematical Modeling, 1<sup>st</sup> ed., Mineola: Dover Publications, 256 p.
- DA LUZ JAM. 2005. Conversibilidade entre Distribuições Probabilísticas Usadas em Modelos de Hidrociclones. Rev Esc Minas 58(1): 89-93.
- EDIL TB, BENSON CH & BAREITHER CA. 2007. Determination of Shear Strength Values for Granular Backfill Material Used by the Wisconsin Department of Transportation. Final report: Wisconsin.
- EPSTEIN B. 1948. Logarithmic Normal Distribution in Breakage of Solids. Ind Eng Chem 40(12): 2289-2291.
- GHASEMI A, CHAYJAN RA & NAJAFABADI HJ. 2018. Optimization of Granular Waste Production Based on Mechanical Properties. Waste Manage 75: 82-93.

HUNGER M & BROUWERS HJH. 2009. Flow Analysis of Water-powder Mixtures: Application to Specific Surface AREA and Shape factor. *Cement Concrete Comp* 31(1): 39-59.

KING RP. 2001. *Modeling and Simulation of Mineral Processing Systems*, 1<sup>st</sup> ed. Boston: Elsevier, 416 p.

LIU X, QU S & HUANG J. 2019. Relationship Between Physical Properties and Particle-size Distribution of Geomaterials. *Constr Build Mater* 222: 312-318.

MOHAMMADI MH & MESKINI-VISHKAEI. 2012. Predicting the Film and Lens Water Volume Between Soil Particles Using Particle Size Distribution Data. *J Hydrol* 475: 403-414.

NASTA P, KAMAI T, CHIRICO GB, HOPMANS JW & ROMANO N. 2009. Scaling Soil Water Retention Functions Using Particle-size Distribution. *J Hydrol* 374(3-4): 223-234.

ORR JR C & DALAVALLE JM. 1959. *Fine Particle Measurement: Size, Surface, and Pore Volume*. New York: Macmillan, 353 p.

OUCHLYAMA N & TANAKA T. 1986. Porosity Estimation from Particle Size Distribution. *Ind Eng Chem Fundam* 25(1): 125-129.

VALADARES TN & DA LUZ JAM. 2004. Porosidade de sistemas polidispersos compactados. In: XX ENTMMME - Encontro Nacional de Tratamento de Minérios e Metalurgia Extrativa. *Proceedings...* Criciúma, p. 235-242.

#### How to cite

LOPES PFT, LUZ JAM & MILHOMEM FO. 2020. Specific surface area of polydispersions as a function of size distribution sharpness. *An Acad Bras Cienc* 92: e20191407. DOI 10.1590/0001-3765202020191407.

*Manuscript received on November 19, 2019;  
accepted for publication on February 10, 2020*

#### PAULO FILIPE T. LOPES

<https://orcid.org/0000-0001-7320-3093>

#### JOSÉ AURÉLIO M. DA LUZ

<https://orcid.org/0000-0002-7952-2439>

#### FELIPE O. MILHOMEM

<https://orcid.org/0000-0002-9830-8374>

Federal University of Ouro Preto, School of Mines, Campus UFOP, Bauxita, 35400-000 Ouro Preto, MG, Brazil

Correspondence to: **José Aurélio Medeiros da Luz**  
E-mail: [jaurelio@ufop.edu.br](mailto:jaurelio@ufop.edu.br)

#### Author contributions

Paulo Filipe Trindade Lopes: mathematical simulation, methodology, validation, formal analysis, investigation, and writing – original draft. José Aurélio Medeiros da Luz: conceptualization, formal analysis; resources, and writing – original draft, review and editing, supervision. Felipe de Orquiza Milhomem: mathematical simulation, writing – review and editing.

